Electronic Supplementary Information

Mediator and Co-catalysts-Free Direct Z-Scheme Composite of Bi_2WO_6/Cu_3P for Solar-water splitting

Ali Rauf,[a,b] Ma Ming,[c] Sungsoon Kim,[d] Md. Selim Arif Sher Shah,[a] Chan-Hwa Chung,[a] Jong Hyeok Park[c]* and Pil J. Yoo[a,e]*

[a].School of Chemical Engineering, Sungkyunkwan University (SKKU), Suwon 16419, Republic of Korea.

[b].Department of Chemical Polymer & Composite Material Engineering, University of Engineering & Technology, KSK Campus, Lahore, Pakistan.

[c].Department of Chemistry, The Hong Kong University of Science and Technology, Hong Kong, China

[d].Department of Chemical and Biomolecular Engineering, Yonsei University, Seoul 03722, Republic of Korea

[e].SKKU Advanced Institute of Nanotechnology (SAINT), Sungkyunkwan University (SKKU), Suwon 16419, Republic of Korea.

Contents

Tables

Figures

References

Examples of failed cases for the synthesis of composites.

In the case of Bi_2WO_6/Cu_3P composite, both cases were tried where Cu_3P and Bi_2WO_6 were used as parent materials and an attempt was made to synthesize second material over parent material to ensure hybridization between two materials. Initially, Cu_3P was used as parent material and was synthesized first using hydrothermal approach and Bi_2WO_6 was planned to synthesized over it by carrying out the sequence of two hydrothermal reactions, after second hydrothermal reaction for composite formation. However, Cu_3P could not retain its crystallography and changed to $BiPO_4$ as shown in Fig. S1a. The incoming Bi^{3+} ions from $Bi(NO_3)_3.5H_2O$ and tungstate ion (WO_4^{2-}) from Na_2WO_4, attacked parent material, i.e. Cu_3P and made $BiPO_4$.

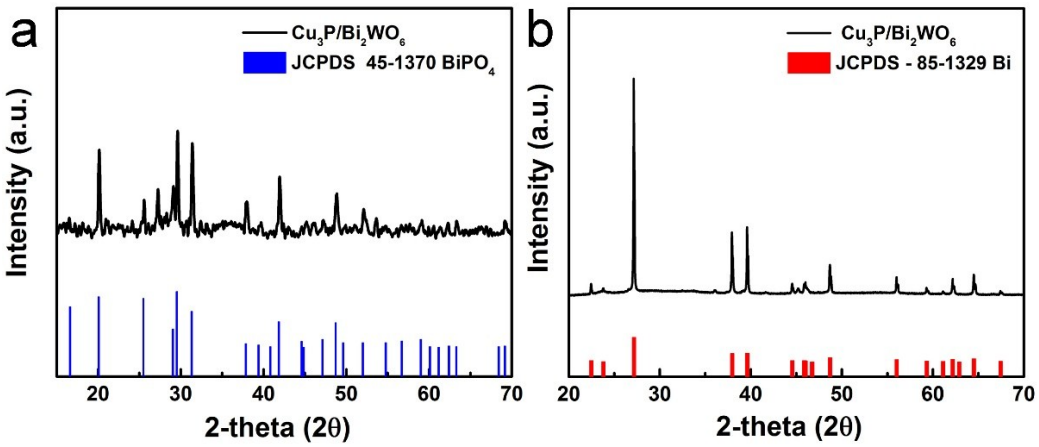

Fig. S1 Two failed synthesis cases (a) When Cu_3P was used as parent material and Bi_2WO_6 was synthesized over it (b) When Bi_2WO_6 was used as parent material and Cu_3P was synthesized over it.

Similarly, in another case, where Bi_2WO_6 was used as parent material, Bi_2WO_6 was synthesized first hydrothermally and then the second hydrothermal reaction was carried out, using CuCl and red P as precursors for Cu and P, respectively, for the synthesis of Bi_2WO_6/Cu_3P composite, the end product is a metallic Bi as shown in Fig. S1b. the plausible reason for the reduction Bi_2WO_6 to Bi metal can be the strong reducing tendency of red P.[1]

The possible solution could be use of any other phosphorus precursor like yellow P or sodium hypophosphite NaH_2PO_2, but they offer certain disadvantageous species like yellow P (highly toxic, very reactive and can easily burn in air due to its low ignition temperature), similarly PH_3 generated as an intermediate product while using NaH_2PO_2, is also toxic.[2,3]

Effect of temperature on the crystallinity of Cu_3P

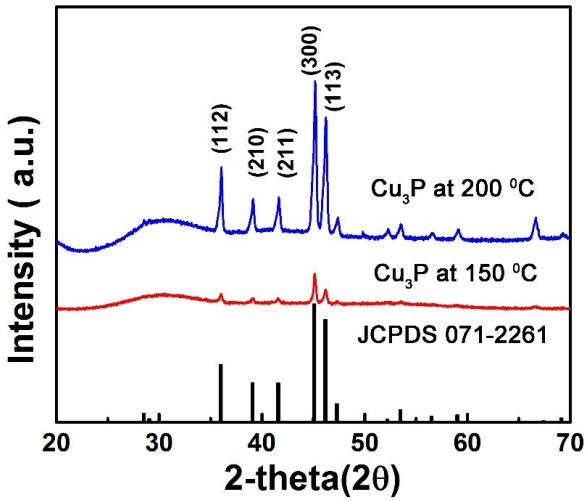

Fig. S2 Effect of temperature on Crystallinity of Cu_3P.

XRD of synthesized Bi_2WO_6

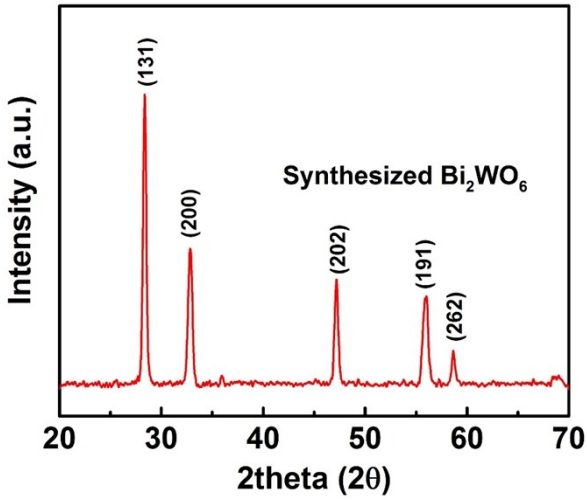

Fig. S3 XRD spectrum of synthesized Bi_2WO_6.

Comparative XPS of Bi_2WO_6(30%)-Cu_3P under different mixing conditions

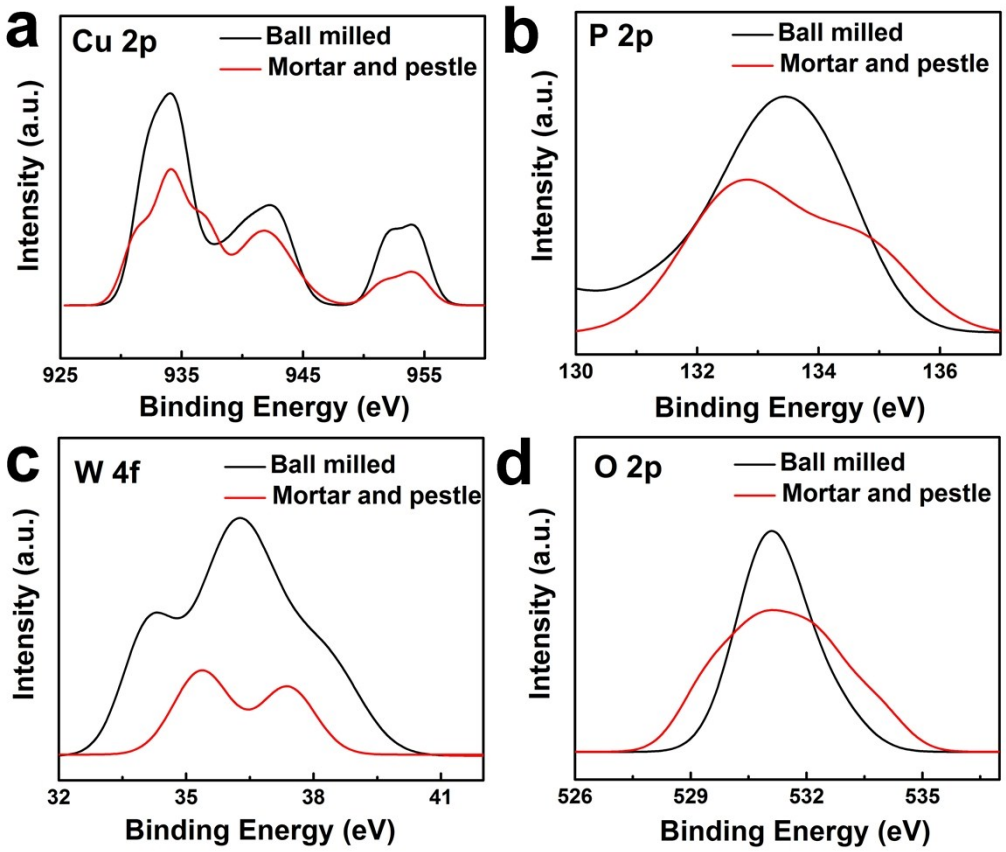

Fig. S4. Comparative XPS with different mixing conditions (a) Core level XPS spectra of Cu 2p (b) Core level XPS spectra of P 2p (c) Core level XPS spectra of W 4f (d) Core level XPS spectra of O 2p

FESEM images for Cu_3P

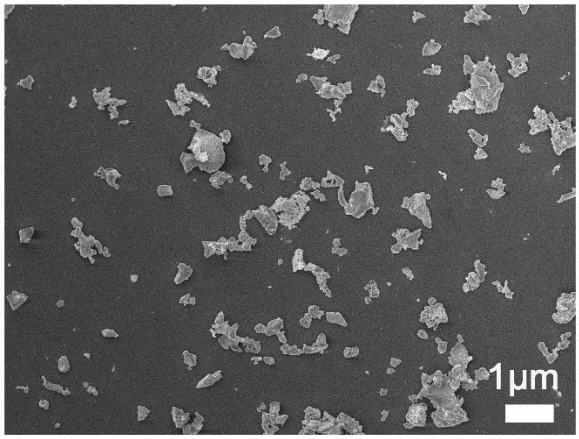

Fig. S5 FESEM image of synthesized Cu_3P.

XRD of Cu_3P under extended ball milling condition

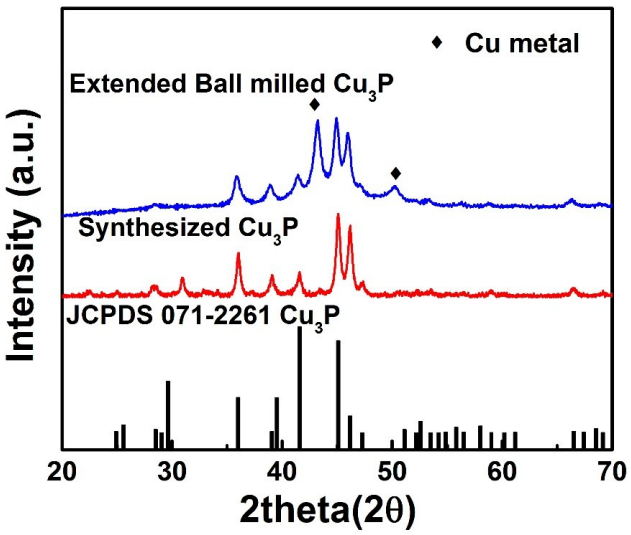

Fig. S6 XRD of Cu3P under extended ball milling conditions

Composite FESEM images

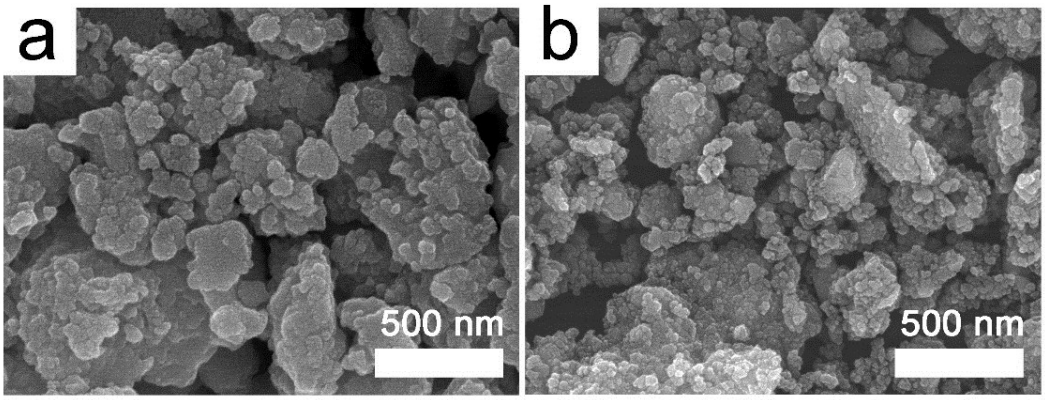

Fig. S7 FESEM images of (a) Bi_2WO_6(20%)-Cu_3P (b) Bi_2WO_6(40%)-Cu_3P

BET surface area and BJH pore size distribution

Table S1 Parameters obtained from N_2 Desorption Isotherm Measurements

Sample	Specific surface area (m^2/g)	Pore diameter (nm)
Cu_3P	11.38	16
Bi_2WO_6(10%)–Cu_3P	9.79	21
Bi_2WO_6(20%)–Cu_3P	6.25	20
Bi_2WO_6(30%)–Cu_3P	5.83	18
Bi_2WO_6(40%)–Cu_3P	4.47	12

Energy levels position calculation

$$E_{VB} = X - E_e + 0.5E_g \qquad (1)$$

Where X is absolute electronegativity of semiconductor expressed as the geometric mean of absolute electronegativity of constituent atoms. The value of X calculated for constituent atoms is by taking arithmetic mean of atomic electron affinity and first ionization energy. Values of X for Bi_2WO_6 and Cu_3P are 6.12 and 4.69, respectively. Similarly, E_e is the energy of free electrons on hydrogen scale i.e. 4.5 eV. Calculated band gaps are 2.8 eV and 1.6 eV for Bi_2WO_6 and Cu_3P. Putting the values in equation 1;

E_{VB} = 3.02 eV for Bi_2WO_6, whereas E_{VB} = 1.02 eV for Cu_3P.

$E_{CB} = E_{VB} - E_g$, then E_{CB} = 0.22 eV for Bi_2WO_6, whereas E_{CB} = – 0.64 eV for Cu_3P.

Valence Band-XPS of Bi_2WO_6 and Cu_3P

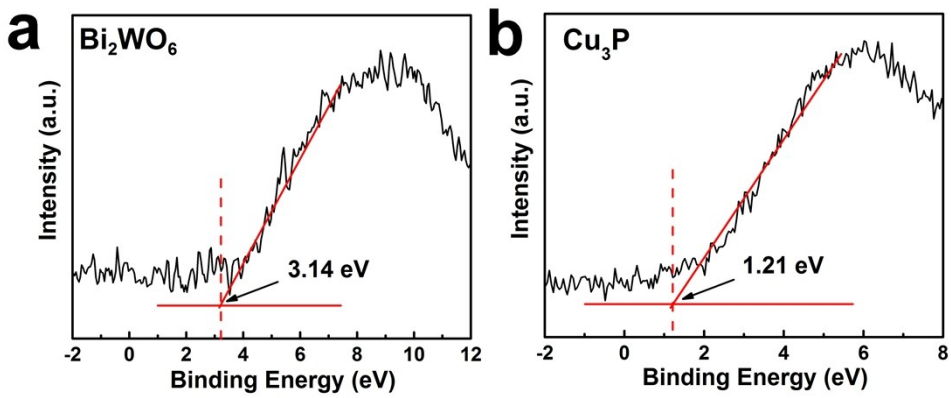

Fig. S8 VB-XPS spectrum (a) Bi_2WO_6 (b) Cu_3P

Energy diagrams of Bi_2WO_6 and Cu_3P

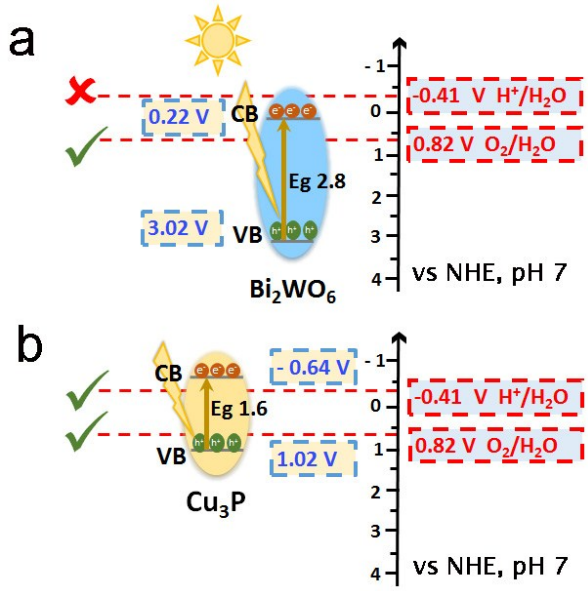

Fig. S9 Energy diagrams (a) Bi_2WO_6 (b) Cu_3P

Comparison of Photocatalytic Activity for all compositions of Bi_2WO_6/Cu_3P

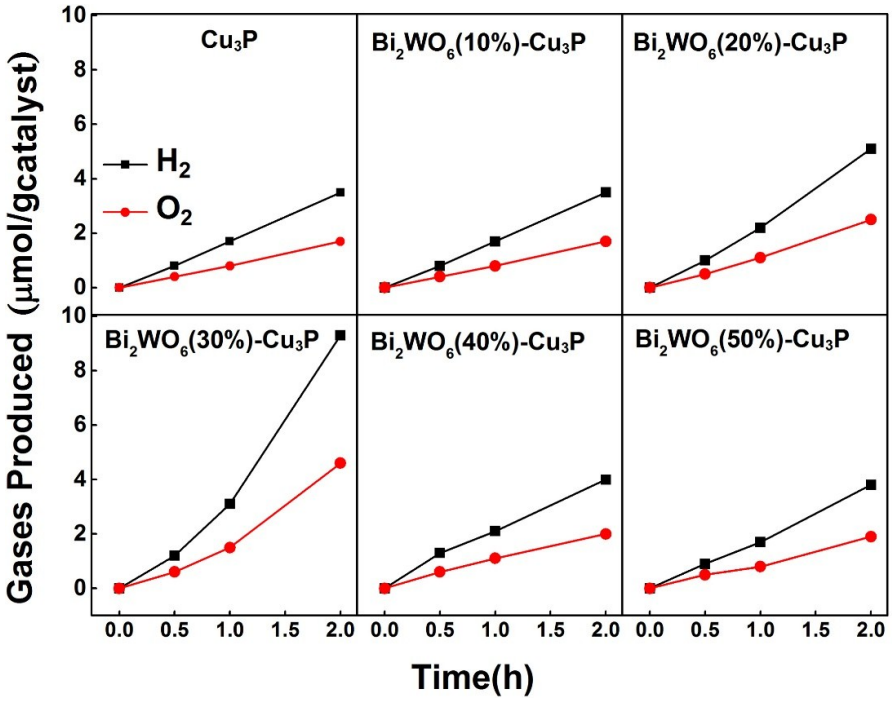

Fig. S10 Time courses of solar-water splitting using different compositions of Bi_2WO_6/Cu_3P. Reaction conditions were, 100 mg photocatalysts were dispersed in 80 ml 0.5M Na_2HPO_4/NaH_2PO_4 buffer solution. Illumination was provided by AM 1.5G simulated sunlight with 100 mW cm^{-2}.

Turn over number (TON) for Cu_3P

Based on amount of products formed i.e. moles of H_2 and O_2 produced are 1.7 and 0.8 μmoles respectively and surface area of Cu_3P which is 11.38m^2/g produced are 3.2×10^{-7} and 1.6×10^{-7} respectively.

Table S2. Comparison study between the Cu_3P and Bi_2WO_6-Cu_3P photocatalyst in this work and previously reported photocatalysts for solar-water splitting

Material	Light Source (wavelength)	Presence of Mediator/ Co-catalysts	Overall Solar-water Splitting		Reference
			H_2 Production μmol/h	O_2 Production μmol/h	
In0.90Ni0.10TaO4	Xe lamp (>400 nm)	Yes	16.6	8.3	*Nature* **2001**, *414*, 625–627.
Pt/WO_3:mZrO_2/TaON	Xe lamp (>400 nm)	Yes	4.2	2	*Bulletin of the Chemical Society of Japan* **2008**, *81*, 927–937.
Cu_2O@ZnCr-LDH	Xe lamp (> 400 nm)	Yes	0.9	0.4	*Nano Energy* **2017**, *32*, 463–469.
Ta_3N_5/$BaTaO_2N$	Xe lamp (>400 nm)	Yes	0.6	0.3	*Chem. Sci.* **2017**, *8*, 437–443.
$BiVO_4$/RGO/ Ru/$SrTiO_3$:Rh	Xe lamp (>400 nm)	Yes	1.1	0.6	*Journal of the American Chemical Society* **2011**, *133*, 11054–11057.
Cr_2O_3/Ru-modified $SrTiO_3$:La,Rh/Au/$BiVO_4$	Xe lamp (Full range)	Yes	1.9	0.9	*Nature Materials* **2016**, *15*, 611–615.
Quantum Sized $BiVO_4$	Xe lamp (Full range)	No	0.2	0.1	*ACS Catal.*, ***2014,*** *4, 3498–3503*
Cu_3P	**Xe lamp (Full range)**	**No**	**1.7**	**0.8**	**This work**
Bi_2WO_6-Cu_3P	**Xe lamp (Full range)**	**No**	**4.6**	**2.3**	**This work**

Photoluminescence

Electron-hole recombination rate was investigated using photoluminescence spectra. The peak intensities in PL spectra have a direct relation with electron-hole recombination rate. PL spectra were measured for all composite samples and Cu_3P was used as a reference sample as shown in Fig. S12. The excitation wavelength was chosen at 765 nm which directly corresponds to the band gap of Cu_3P i.e. 1.6 eV calculated from UV-vis spectrophotometry. So Cu_3P showed its intrinsic emission peak at 786 nm. It is observed the trend shown by proposed composite is opposite to what is general in case of conventional heterostructure as recombination is suppressed for that case.[4,5] However, here the peak intensity increases as compared to the parent material which clearly highlighting the fact, electron-hole recombination has increased in case of composite. Increased electron-hole recombination in case of composite as compared to parent material is a general indicator for Z-scheme formation.[6,7,8] A slight peak shift is also observed which is probably due to the hybridization between Cu_3P and Bi_2WO_6. [4,9]

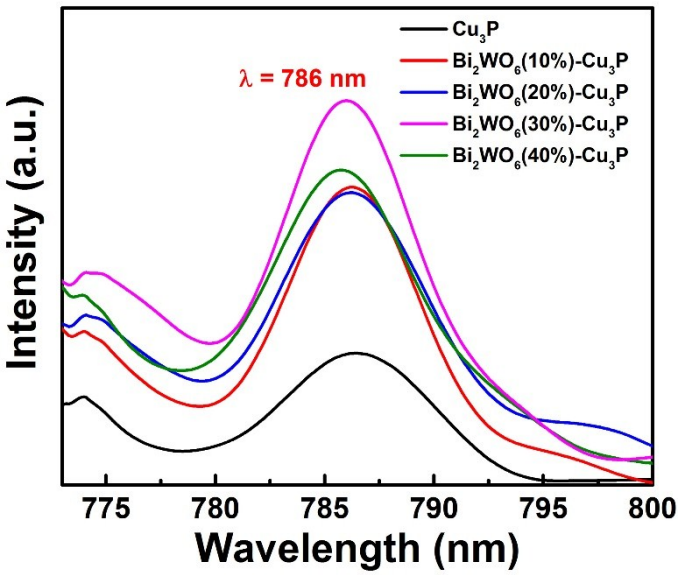

Fig. S11 PL spectrum of different samples

References

(1) Rosenstein, L. RED PHOSPHORUS AS A REDUCING AGENT. *Journal of the American Chemical Society* **1920**, *42*, 883–889.

(2) DIAZ-RIVERA, RS, COLLAZO PJ, PONS ER, T. M. Acute Phosphorus Poisoning in Man: A Study of 56 Cases. *Medicine (Baltimore)* **1950**, *29*, 269–298.

(3) Eismann, F.; Glindemann, D.; Bergmann, A.; Kuschk, P. Effect of Free Phosphine on Anaerobic Digestion. *Water Research* **1997**, *31*, 2771–2774.

(4) Rauf, A.; Sher Shah, M. S. A.; Choi, G. H.; Humayoun, U. Bin; Yoon, D. H.; Bae, J. W.; Park, J.; Kim, W.-J.; Yoo, P. J. Facile Synthesis of Hierarchically Structured Bi_2S_3 /Bi_2 WO_6 Photocatalysts for Highly Efficient Reduction of Cr(VI). *ACS Sustainable Chemistry & Engineering* **2015**, *3*, 2847–2855.

(5) Zhang, Z.; Wang, W.; Wang, L.; Sun, S.; Case, N. S. A.; Bi, B. S.; Zhang, Z.; Wang, W.; Wang, L.; Sun, S. Enhancement of Visible-Light Photocatalysis by Coupling with Narrow-Band-Gap Semiconductor: A Case Study on Bi_2S_3/Bi_2WO_6. *ACS Applied Materials and Interfaces* **2012**, *4*, 593–597.

(6) Ye, R.; Fang, H.; Zheng, Y.-Z.; Li, N.; Wang, Y.; Tao, X. Fabrication of $CoTiO_3$/g-C_3N_4 Hybrid Photocatalysts with Enhanced H_2 Evolution: Z-Scheme Photocatalytic Mechanism Insight. *ACS Applied Materials & Interfaces* **2016**, *8*, 13879–13889.

(7) Chen, S.; Hu, Y.; Meng, S.; Fu, X. Study on the Separation Mechanisms of Photogenerated Electrons and Holes for Composite Photocatalysts G-C_3N_4-WO_3. *Applied Catalysis B: Environmental* **2014**, *150–151*, 564–573.

(8) Li, H.; Hu, T.; Zhang, R.; Liu, J.; Hou, W. Preparation of Solid-State Z-Scheme Bi2MoO6/MO (MCu, $Co_{3/4}$, or Ni) Heterojunctions with Internal Electric Field-Improved Performance in Photocatalysis. *Applied Catalysis B: Environmental* **2016**, *188*, 313–323.

(9) Rauf, A.; Arif Sher Shah, M. S.; Lee, J. Y.; Chung, C.; Bae, J. W.; Yoo, P. J. Non-Stoichiometric SnS Microspheres with Highly Enhanced Photoreduction Efficiency for Cr(VI) Ions. *RSC Adv.* **2017**, *7*, 30533–30541.